



Published in final edited form as:

Curr Biol. 2023 March 27; 33(6): 1036–1046.e6. doi:10.1016/j.cub.2023.01.059.

Increased Alcohol Dehydrogenase 1 activity promotes longevity

Abbas Ghaddar^{1,†}, Vinod K. Mony^{1,†}, Swarup Mishra^{1,2}, Samuel Berhanu¹, James C. Johnson², Elisa Enriquez-Hesles², Emma Harrison¹, Aaroh Patel¹, Mary Kate Horak^{1,3}, Jeffrey S. Smith², Eyleen J. O'Rourke^{1,3,4,5,*}

¹Department of Biology, College of Arts and Sciences, University of Virginia, Charlottesville, VA 22903, USA.

²Department of Biochemistry and Molecular Genetics, University of Virginia School of Medicine, Charlottesville, VA 22903, USA.

³Department of Cell Biology, School of Medicine, University of Virginia, Charlottesville, VA 22903, USA.

⁴Robert M. Berne Cardiovascular Research Center, School of Medicine, University of Virginia, Charlottesville, VA 22903, USA.

⁵Lead contact.

Abstract

Several molecules can extend healthspan and lifespan across organisms. However, most are upstream signaling hubs or transcription factors orchestrating complex anti-aging programs. Therefore, these molecules point to but do not reveal the fundamental mechanisms driving longevity. Instead, downstream effectors that are necessary and sufficient to promote longevity across conditions or organisms may reveal the fundamental anti-aging drivers. Towards this goal, we searched for effectors acting downstream of the transcription factor EB (TFEB), known as HLH-30 in *C. elegans*, because TFEB/HLH-30 is necessary across anti-aging interventions and its overexpression is sufficient to extend *C. elegans* lifespan and reduce biomarkers of aging in mammals including humans. As a result, we present an Alcohol-dehydrogenase Mediated anti-Aging Response (AMAR) that is essential for *C. elegans* longevity driven by HLH-30 overexpression, caloric restriction, mTOR inhibition, and insulin-signaling deficiency. The sole overexpression of ADH-1 is sufficient to activate AMAR, which extends healthspan and lifespan by reducing the levels of glycerol – an age-associated and aging-promoting alcohol. *Adh1* overexpression is also sufficient to promote longevity in yeast, and *adh-1* orthologs are induced in

*Corresponding author: ejourourke@virginia.edu.

Author contributions

The study was conceived and designed by AG and EJO. *C. elegans* experiments were performed by AG, VKM, SB, EH, AP, MKH and EJO and analyzed by AG, VKM and EJO. Yeast experiments were performed and analyzed by SM, JCJ, EEH and JSS. The manuscript was written by AG, VKM and EJO.

†These authors contributed equally to this work.

Publisher's Disclaimer: This is a PDF file of an unedited manuscript that has been accepted for publication. As a service to our customers we are providing this early version of the manuscript. The manuscript will undergo copyediting, typesetting, and review of the resulting proof before it is published in its final form. Please note that during the production process errors may be discovered which could affect the content, and all legal disclaimers that apply to the journal pertain.

Declaration of interests

The authors declare no competing interests.

calorically restricted mice and humans, hinting at ADH-1 acting as an anti-aging effector across phyla.

Introduction

Advances in the field of aging include the discovery of several genetic and biochemical pathways that shorten or extend lifespan. However, the molecules found to be necessary and sufficient to extend health and lifespan have mostly been upstream signaling hubs (*e.g.* mTOR) or intermediate transcription factors (*e.g.* FOXO/DAF-16). Therefore, it remains unclear whether there are downstream effectors that are necessary and sufficient for longevity. This is relevant, as downstream molecules with robust anti-aging effects may reveal the fundamental mechanisms that determine the rate of aging and may be safer and more effective geroprotective targets.

An attractive approach to the discovery of downstream effectors of longevity is the study of the transcription factors (TFs) responsible for activating anti-aging programs in multiple pro-longevity conditions. A prominent anti-aging TF in this class is the Transcription Factor EB (TFEB). Activation of TFEB, and its *C. elegans* ortholog HLH-30, is necessary to extend healthspan and lifespan across anti-aging interventions^{1,3}. Furthermore, activating HLH-30/TFEB is sufficient to promote longevity and reduce biomarkers of aging across organisms^{1,4-8}. As a master regulator of autophagy and lysosomal biogenesis⁹, the current model states that HLH-30/TFEB extends health and lifespan through the activation of autophagy¹, a cell rejuvenating process that is also thought to be required across anti-aging interventions and organisms¹⁰⁻¹⁴.

While investigating the potential role of autophagy in the *hlh-30* dependent longevity of the *mxl-3 C. elegans* mutant, we found that the current model has exceptions. Since *mxl-3*-driven longevity requires the activity of *hlh-30*, HLH-30/TFEB is the master regulator of autophagy, and autophagy is thought to be universally required for longevity, we hypothesized that *hlh-30* was promoting longevity in the *mxl-3* mutants through the activation of autophagy. However, contrary to expectation, we found that autophagy is not activated in the *mxl-3* mutant, and that neither autophagy nor lysosomal activity² are required for the longevity phenotype observed in these mutant animals. Therefore, *mxl-3* longevity is *hlh-30*-dependent but autophagy-independent. Instead, we found the gene encoding the Alcohol DeHydrogenase ADH-1 induced in *mxl-3* and other *hlh-30*-dependent anti-aging interventions, including caloric restriction (*eat-2* mutants), insulin-signaling deficiency (*daf-2* deficient) and mTOR-inhibition. More importantly, *adh-1* is necessary for the longevity phenotype of all these anti-aging interventions, and ADH-1 overexpression is sufficient to extend *C. elegans* lifespan. We propose that ADH-1 extends lifespan through metabolizing the otherwise toxic alcohol glycerol, which accumulates with age. Finally, we present evidence suggesting that ADH-1's anti-aging capacity may be conserved across species. Altogether, we establish ADH-1 as an effector of longevity acting downstream of multiple anti-aging interventions and propose it as a druggable enzyme whose activation may suffice to promote healthspan and lifespan in organisms ranging from yeast to humans.

Results

Autophagy and lysosomal activity can be dispensable for *hlh-30*-dependent longevity

C. elegans mutants for the helix-loop-helix transcription factor *mxl-3* are long-lived. This longevity phenotype is suppressed by inactivation of the gene encoding the transcription factor HLH-30 (known as TFEB in mammals) (Figure 1A; Data S1A). Given that HLH-30/TFEB is known as the master regulator of autophagy and lysosomal biogenesis, we hypothesized that *mxl-3*'s longevity was also dependent on autophagic and lysosomal activity. However, the levels of autophagy in the long-lived *mxl-3* animals are normal at the transcriptional (Figure S1A), biochemical (Figure S1B) and cytological levels (Figure S1C). Most importantly, (i) post-developmental inactivation by RNAi of two autophagy genes that are lethal when mutated, *lgg-1* (a.k.a. Atg-8 or LC3) and *bec-1* (Figure S1D; Data S1B), (ii) loss-of-function mutation of the non-lethal autophagy gene *atg-18* (Figure 1B and Data S1C), and (iii) chemical inhibition of all lysosomal enzymes with chloroquine do not suppress or rescue *mxl-3*'s longevity, respectively (Figure S1E; Data S1C). In fact, post-developmental RNAi against *atg-18*, *lgg-1* and *bec-1* and post-developmental administration of chloroquine further increased *mxl-3* lifespan (Figure S1D, Figure S1E and Data S1B and S1C), demonstrating that the treatments worked but, more importantly, that autophagic and lysosomal activity are not always necessary for longevity.

adh-1 mediates HLH-30-driven longevity

To identify alternative effectors driving HLH-30-mediated longevity, we mined published *hlh-30* mutant transcriptomics¹⁵, and HLH-30 overexpression (HLH-30^{OE}) transcriptomics¹⁶, proteomics¹⁶, and ChIP-Seq studies¹⁷. The top gene that met the following criteria: (i) mRNA and protein dysregulated in the *hlh-30* mutant and HLH-30^{OE} strains, respectively, and (ii) a hit in the HLH-30 ChIP-seq study, was K12G11.3, which encodes for the alcohol dehydrogenase ADH-1. We therefore used the *mxl-3* mutant model to investigate *adh-1*'s potential role in *hlh-30*-driven longevity. In line with ADH-1 playing a role in *hlh-30*-mediated longevity, *adh-1* was induced in the *mxl-3* mutant animals in an *hlh-30*-dependent manner (Figure 1C). More importantly, loss-of-function mutation of *adh-1* suppressed *mxl-3*'s longevity phenotype (Figure 1D & Data S1D). Therefore, unlike autophagy, the activity of the alcohol dehydrogenase ADH-1 is necessary for *hlh-30*-dependent *mxl-3* longevity.

We then investigated whether *adh-1* played a role in HLH-30-mediated longevity beyond the *mxl-3* model. In *C. elegans*, the sole overexpression of HLH-30 is sufficient to extend lifespan¹. We confirmed this result, while also finding the pro-longevity effect of overexpressing HLH-30 to be more pronounced in the *C. elegans* line OP433¹⁸ than in the previously described MAH235 and MAH240 lines¹ (Data S1D). This, in addition to OP433 being the *C. elegans* line used in the referred ChIP-Seq and proteomics analyses, persuaded us to use OP433 as the model for HLH-30 hyperactivation throughout this study (hereinafter referred to as HLH-30^{OE}; please refer to the Methods section “*C. elegans* lifespan assays” for experimental conditions). In line with ADH-1 being an anti-aging effector downstream of HLH-30, we found *adh-1* induced in HLH-30^{OE} animals (Figure 1E). More importantly, loss-of-function mutation of *adh-1* fully suppressed HLH-30^{OE} longevity (Figure 1F, Figure

S2, Data S1D & Data S1E). This result indicates that *adh-1* plays a critical role in HLH-30-driven longevity in contexts beyond the loss of *mxl-3*.

ADH-1 is necessary and sufficient to promote longevity

Given that *hlh-30* is necessary for longevity across anti-aging interventions¹, we then tested whether *adh-1* similarly contributes to longevity across interventions, namely: (i) caloric restriction through the use of the eating-deficient mutant *eat-2*, (ii) mTOR inhibition through RNAi knockdown of its encoding gene *let-363*, and (iii) reduced insulin signaling through RNAi knockdown of the insulin receptor-encoding gene *daf-2*. Mining published microarray data suggested that *adh-1* is induced in the *eat-2*¹⁹ and *daf-2*^{19,20} models. We confirmed these observations in dedicated transcriptional analyses and, critically, we found that *hlh-30* is necessary for the induction of *adh-1* in all three longevity models (Figure 2A). More importantly, *adh-1* inactivation partially suppressed the extended lifespan of *C. elegans* subject to caloric restriction (Figure 2B & Data S1F) and mTOR deficiency (Figure 2C & Data S1G) and, most strikingly, fully suppressed the extremely long lifespan of the *daf-2*-deficient animals (Figure 2D & Data S1H), demonstrating that *adh-1* is a potent downstream effector of longevity across anti-aging interventions.

Having found that *adh-1* is necessary for lifespan extension across longevity models, we set out to test whether hyperactivating *adh-1* was sufficient to promote longevity. For this, we generated three independent ADH-1 overexpressing *C. elegans* strains (GMW20, GMW21, GMW22 referred to as ADH-1^{OE}). After backcrossing and confirming that all three strains had increased *adh-1* transcript levels (Figure S3A), we found all three to be long-lived relative to the wild-type strain (Figure 2E, Figure S3C, Data S1I & Data S1J). We also found that aged ADH-1^{OE} animals show improved locomotor endurance compared to their age-matched WT counterparts (Figure 2F), suggesting that hyperactivation of ADH-1 may also extend healthspan. Therefore, ADH-1 is not only necessary for longevity across anti-aging interventions, but it is also sufficient to extend lifespan and likely healthspan.

Next, we characterized the ADH-1^{OE} animals. We found no difference in the size (Figure S3D) or in the feeding rate (pharyngeal pumping) (Figure S3E) of ADH-1^{OE} animals compared to WT animals, suggesting that overexpressing ADH-1 does not cause caloric restriction in *C. elegans*. The defecation rate of ADH-1^{OE} animals was also normal (Figure S3F), suggesting normal passage of food through the digestive system. We also sought to determine whether there was a trade-off between extended lifespan and fertility in ADH-1^{OE} animals, as this tradeoff occurs in several longevity models^{21,22}. Indeed, we found that the ADH-1^{OE} animals exhibit reduced brood size compared to their WT counterparts (Figure S3G and Figure S3H).

ADH-1 promotes longevity by reducing glycerol toxicity

Alcohol dehydrogenases are among the most conserved and studied enzymes due to their biotechnological (*e.g.* wine production) and biomedical relevance (*e.g.* alcohol toxicity). To gain insight into the mechanism through which ADH-1 extends *C. elegans* lifespan, we tested the primary sequence prediction that ADH-1 can metabolize alcohols using a specific *in vivo* alcohol dehydrogenase (AD) assay validated in organisms ranging from

yeast to humans^{23–25}. In this assay, ADs convert allyl-alcohol (AA) into the lethal aldehyde acrolein; hence, higher AD activity leads to higher lethality²⁶. ADH-1^{OE} *C. elegans* showed hypersensitivity to allyl-alcohol (Figure 3A), confirming these animals have increased capacity to metabolize alcohols.

Using scRNA-Seq²⁷ (Figure S4A), we found *adh-1* expressed in the distal tip cells of the gonad, in the marginal and muscle cells of the pharynx (pm3_pm4_pm5 & pm6_pm7), in all body wall muscle cells, and in the anterior intestinal cells. We then used CRISPR/Cas9 to knock-in *wrmScarlet*²⁸ in frame with the coding sequence of *adh-1* to generate a strain carrying *adh-1P::ADH-1::wrmScarlet::adh-1 3'UTR* in the *adh-1* locus. In congruence with the scRNA-Seq expression pattern, we found ADH-1::wrmScarlet expressed in the distal tip, pharynx, body-wall muscle, and the intestinal cells of adult *C. elegans* (Figure 3B, 3C and S4B). At the subcellular level, we noticed that ADH-1 was expressed in droplet-like structures in the intestine, which was intriguing because homologous alcohol dehydrogenases are mainly found in the cytoplasm or in the mitochondria^{29,30}. Co-expression of *adh-1P::ADH-1::wrmScarlet::adh-1 3'UTR* with the intestinal lipid droplet (LD) reporter *daf-22P::PLIN1::GFP*³¹ showed that ADH-1 colocalizes with LDs (Figure 3C).

Given that (i) ADH-1 is an alcohol dehydrogenase expressed in close proximity to LDs, (ii) the major molecular class present in LDs is triglycerides, which are composed of fatty acids and the alcohol glycerol, and (iii) glycerol had previously been shown to reduce lifespan³², we hypothesized that ADH-1 extends *C. elegans* lifespan by reducing the levels of the aging-promoting alcohol glycerol. In support of this hypothesis, we found that wild-type *C. elegans* accumulate glycerol as they age (Figure 3D), and that ADH-1^{OE} animals show reduced glycerol levels relative to wild-type worms (Figure 3E) and are resistant to the pro-aging effect of glycerol (Figure 3F & Data S1K & S1L). We also performed a food choice assay to determine whether ADH-1^{OE} animals show a differential attraction to glycerol. Wild-type *C. elegans* showed no preference for glycerol at the doses used in the lifespan assays (0.04% and 0.4%), and we observed no differences between the ADH-1^{OE} and WT genotypes (Figure S3I & S3J); therefore, ADH-1^{OE} animals are not living longer because they are avoiding the glycerol or the glycerol-embedded food. Altogether, the data support a model in which wild-type *C. elegans* accumulate glycerol as they age which results in reduced lifespan. However, when *adh-1* is induced, as in the HLH-30-dependent longevity models, glycerol levels are lower, and lifespan is extended (schematic model in Figure 4F). We name this lifespan-extending mechanism Alcohol dehydrogenase Mediated Anti-aging Response or AMAR, which in Sanskrit means immortal. A prediction of the AMAR model is that HLH-30^{OE} animals would have reduced glycerol levels relative to WT worms, and that this reduction would depend on the activity of ADH-1. Indeed, we find that HLH-30^{OE} animals have reduced glycerol levels compared to WT worms, and that this reduction is suppressed when *adh-1* is mutated (Figure 3G).

ADH-1 mediated longevity requires ALH activity

Another prediction of the AMAR model is that increased glycerol metabolism by ADH-1 will lead to increased levels of another toxic and aging-promoting metabolite,

glyceraldehyde³³. We therefore hypothesized that *adh-1*-driven longevity would require aldehyde dehydrogenase (ALH) activity to convert glyceraldehyde into its non-toxic salt, glycerate. *C. elegans* has over 12 aldehyde dehydrogenase encoding genes. Therefore, to determine whether ALH activity is required for ADH-1 mediated longevity, we used the ALH-specific inhibitor cyanamide^{34,35}. Treating ADH-1^{OE} worms with cyanamide fully rescued their longevity phenotypes (Figure 4A, Figure S3C & Data S1I and S1J). Furthermore, cyanamide suppressed the extended lifespan of the *hlh-30*-dependent longevity models *mxl-3* (Figure 4B & Data S1M), *eat-2* (Figure 4C & Data S1F), *daf-2* (Figure 4D & Data S1H), and, as predicted by the model, HLH-30^{OE} animals (Figure 4E, Figure S2 & Data S1E and S1M). Therefore, concerted alcohol- and aldehyde-dehydrogenase function is required for lifespan extension across anti-aging interventions.

ADH-1 is a conserved anti-aging effector

Having found that *adh-1* is necessary and sufficient for longevity in *C. elegans*, we mined the literature in search for evidence of conservation. We found studies in yeast demonstrating that alcohol dehydrogenase (AD) activity decreases with age³⁶. On the other hand, here we show that Adh1 protein levels increase in yeast subject to caloric restriction (Figure 5A) and, more importantly, using an estradiol-based system to increase Adh1 levels (Figure S5A), we show that Adh1 promotes a dose-dependent increase in yeast chronological lifespan (Figure 5B). Adh1's necessity and sufficiency to extend lifespan in *C. elegans*, and sufficiency to extend yeast lifespan, suggest that this enzyme's anti-aging role might be conserved across species.

To test this notion, we mined the literature for transcriptomics analyses of mammals subject to two life-extending treatments: fasting or caloric restriction. Data S1S lists all the studies we found in which *Adh1*, or other close homologs of *C. elegans' adh-1* such as *Adh4*, *Adh5*, and *Sord*, were induced (see Data S1S). Briefly, we found 18 transcriptomic datasets where the mouse orthologs of *C. elegans adh-1* were induced in calorically restricted humans. Similarly, we found 6 transcriptomic datasets where the human orthologs of *C. elegans adh-1* are induced in calorically restricted humans. Altogether, the data demonstrate that ADH-1 is an anti-aging effector common to multiple anti-aging interventions and suggest that it may promote longevity across species.

Discussion

The transcription factor HLH-30, known as Mitf in flies and TFEB in mammals, has been the focus of intense study. At the molecular level, HLH-30/TFEB is known as the master regulator of lysosomal biogenesis and autophagy because *in vitro* in cellular models^{37,38} and *in vivo* in animal models, HLH-30/TFEB is necessary and sufficient for the expansion of the lysosomal compartment and the activation of autophagy^{3,9,39,40}. At the organismal level, HLH-30/TFEB promotes survival to acute stress⁴¹⁻⁴³ and reduces the incidence and severity of the symptoms of aging across model systems^{6-8,44}, and, in *C. elegans*, *hlh-30* is necessary for longevity^{1,3}. Autophagy, a downstream output of HLH-30/TFEB activation is also thought to be indispensable for extended lifespan^{12,13}. Therefore, it was reasonable to hypothesize that the broad requirement of HLH-30/TFEB to promote survival was due

to its role in the activation of the cellular rejuvenating process of autophagy. However, work from the Antebi lab showed that the months-long survival of the germline in *C. elegans* undergoing starvation, a survival program known as adult reproductive diapause (ARD), depends on the activity of HLH-30 but not of autophagy⁴⁵. This indicates that autophagy is not always necessary for HLH-30-driven survival to stress. Furthermore, enhanced autophagy may not be sufficient to promote long-term survival. For instance, *C. elegans* carrying a hypomorphic mutation in the gene encoding the insulin receptor *daf-2* are long lived, and loss-of-function mutation of the transcription factor *daf-16* (mammalian *Foxo*) fully suppresses this longevity phenotype. However, *daf-16* does not suppress the high levels of autophagy observed in the *daf-2* mutant worms¹¹. Therefore, *daf-2;daf-16* double mutant worms have high-levels of autophagy but are not long-lived. Together, the ARD and *daf-2;daf-16* studies suggest that autophagy is neither universally required nor sufficient to promote long-term survival.

By contrast, HLH-30/TFEB seems necessary across anti-aging interventions and sufficient to reduce the burden of aging across species. Therefore, common downstream effectors of longevity could be discovered by investigating *hlh-30*'s mechanism of lifespan extension. To identify these effectors, we here characterized the *C. elegans* mutant *mxl-3*. On one side, we chose this anti-aging intervention because the *mxl-3*'s longevity phenotype is completely suppressed by loss of *hlh-30* function. On the other hand, distinct from other *hlh-30*-dependent anti-aging interventions (*e.g.*, mTOR or insulin receptor inactivation) that perturb upstream signaling hubs with broad cellular impacts, *mxl-3* encodes for a transcription factor with the same DNA-binding site as HLH-30³. Therefore, the study of the *mxl-3-hlh-30* longevity model was more likely to point us to critical anti-aging effectors acting downstream of HLH-30.

The initial characterization of the *mxl-3 C. elegans* mutant showed that its longevity phenotype does not require autophagy. It is worth noting here that, distinct from some previous studies, we used post-developmental RNAi and post-developmental chloroquine treatment to test the contribution of the autophagy and lysosomal machinery to *mxl-3*'s longevity. Post-developmental treatment was necessary because inactivation of autophagy during development leads to several developmental defects ranging from developmental arrest^{46,47} to altered adult physiology (*e.g.*, reduced fat accumulation⁴⁸). We found that post-developmental RNAi against *atg-18*, *lgg-1*, and *bec-1*, as well as complete inhibition of lysosomal activity with chloroquine, further increased the lifespan of the *mxl-3* mutant worms. Future studies may investigate whether this enhanced longevity is due to a hormetic effect by which reduced autophagy promotes the activation of alternative cellular homeostatic processes such as the heat-shock response, proteasomal function, or other compensatory responses to dysfunctional autophagy, as previously observed *in vitro*^{49,50}. Furthermore, our observations are in line with previous studies showing that post-developmental inactivation of autophagy can extend *C. elegans* lifespan⁵¹ and a study showing that chloroquine treatment can increase lifespan in rats, in part through the modulation of autophagy⁵². The results presented here indicate that longevity is possible in the absence of enhanced autophagy and that the master regulator of autophagy, HLH-30/TFEB, can promote longevity by mechanisms that are autophagy-independent.

Our search for alternative mechanisms of longevity orchestrated by HLH-30 pointed us to the alcohol dehydrogenase ADH-1. In the intestine of *C. elegans*, we found that ADH-1 localizes to the surface of lipid droplets (LDs). The main component of LDs are triglycerides, and triglycerides are composed of fatty acids and glycerol. Although most of the attention given to lipotoxicity focuses on the detrimental effects of free fatty acids, the alcohol glycerol can also be toxic. In fact, glycerol has been shown to shorten *C. elegans* lifespan³², and we show here that it normally accumulates in aging worms. Therefore, ADH-1 is in the right place in the cell to access and metabolize glycerol and, therefore, reduce the pro-aging effects of this naturally occurring alcohol (working model in Figure 4F). In line with this model, ADH-1^{OE} worms have lower levels of glycerol compared to wild type worms and are resistant to the pro-aging effects of glycerol. It is worth noting that ADH-1 overexpression and *adh-1* loss of function mutation do not have opposite phenotypes in *C. elegans*, which is similar to *hlh-30* itself. Loss of *hlh-30* function does not reduce *C. elegans* lifespan^{1,3} while *hlh-30* overexpression promotes longevity. Nevertheless, we here demonstrate that loss of *adh-1* leads to higher levels of glycerol in the HLH-30^{OE} background, which otherwise shows low levels of glycerol. Therefore, ADH-1 activity negatively correlates with the levels of glycerol, and glycerol levels negatively correlate with lifespan. We propose that ADH-1 extends lifespan, at least in part, through alleviating the toxic effects of glycerol likely derived from fat stores that normally increase with age.

Additionally, in line with *adh-1* being a critical downstream effector of HLH-30 longevity, loss of *adh-1* function suppresses the longevity phenotype of all the *hlh-30*-dependent longevity models tested (*mxl-3*, *eat-2*, *daf-2* and mTOR). Interestingly, although loss of *adh-1* function significantly suppresses the extreme longevity phenotype of *daf-2* *C. elegans*, inhibition of the next step in the metabolism of glycerol (aldehyde dehydrogenase) only partially rescued *daf-2* longevity. There are at least two possible interpretations for this observation. From a technical perspective, it is possible that the dose of cyanamide was insufficient to fully inhibit all aldehyde dehydrogenase activity. From a biological perspective, it is possible that ADH-1 contributes to longevity through additional mechanisms.

Interestingly, the longevity models dependent on *adh-1* either mimic fasting conditions (*e.g.*, reduced insulin and mTOR signaling, and HLH-30 overexpression), or reduce food intake (*i.e.*, *eat-2*). Furthermore, the *hlh-30*-dependent but autophagy-independent ARD program of germline-survival is activated in response to fasting⁴⁵. Fasting and caloric restriction are anti-aging interventions effective across species and because ADH-1 is a common mediator of fasting-like anti-aging interventions, we hypothesized that ADH-1 may promote lifespan extension across species. We here confirmed this hypothesis in *Saccharomyces cerevisiae*, where we observed that overexpressing *Adh1* is sufficient to extend chronological lifespan. We also found several studies showing that alcohol-dehydrogenase levels decrease in aging flies, rodents, and humans⁵³⁻⁵⁷, and our mining of published transcriptomics studies of mammals subject to fasting or caloric restriction identified *adh-1* orthologs induced in 18 mouse and 6 human transcriptomic datasets. Furthermore, a meta-analysis of transcriptomic studies of calorically restricted mice, rats, pigs, and rhesus monkeys identified *ADH1* as the most induced gene⁵⁸. A separate meta-analysis of mouse transcriptomic data identified *ADH1* as induced in response to several longevity-promoting interventions including caloric

restriction, every-other-day feeding, and rapamycin treatment⁵⁹. Additionally, comparing the mouse inbred lines C3H and C57BL/6J, showed that C57BL/6J has twice as much liver ADH1 activity⁶⁰ and correspondingly, on average, C57BL/6J mice outlive CH3 by more than 100 days⁶¹. Admittedly, these studies are correlative, however, coupled to our *C. elegans* and yeast causal tests they suggest that *Adh1* may be a universal anti-aging effector. Indeed, two causal studies in mice support this hypothesis. Tissue-specific overexpression of *Adh1* protects mice against neurodegeneration⁶² and cardiac dysfunction⁶³. In summary, the evidence points to the AMAR, as a convergent anti-aging effector acting across longevity programs and possibly across organisms including humans.

EXPERIMENTAL MODEL AND SUBJECT DETAILS

C. elegans strains and husbandry

C. elegans N2 (Bristol, UK), *adh-1* (*ok2799*), *mxl-3* (*ok1947*), *atg-18* (*gk378*), *eat-2* (*ad456*), OP433 [*hlh-30::TY1::EGFP::3xFLAG + unc-119(+)*], MAH235 (sqIs19 [*hlh-30p::hlh-30::GFP + rol-6(su1006)*]) and MAH240 (sqIs17 [*hlh-30p::hlh-30::GFP + rol-6(su1006)*]) were obtained from the Caenorhabditis Genetics Center (CGC). The CRISPR-Cas9 *adh-1*KI strain (PHX2365) and the 3 independent ADH-1^{OE} strains (PHX2888, PHX2889, PHX2890) were generated for this study by SunyBiotech (China). After UV-driven integration, PHX2888, PHX2889, and PHX2890 were backcrossed 3 times; the respective backcrossed strains are referred to as GMW20, GMW21, GMW22. XD3971 strain (xdIs143[P*daf-22::PLIN1::GFP; rol-6(su1006)*]) was a generous gift from Dr. Monica Driscoll and Dr. Xun Huang. Genetic crosses were performed to generate *mxl-3;adh-1*, *mxl-3;atg-18*, HLH-30^{OE}; *adh-1*, and pLIPIN::GFP;*adh-1::wrmScarlet* strains. For maintenance, *C. elegans* were grown at 20°C on NGM plates seeded with *E. coli* strain OP50. All experiments (except the glycerol supplementation aging experiments) including those not involving RNAi were performed using *E. coli* XU363⁶⁴ carrying L4440 (empty vector) or L4440 plus the gene of interest. We used *E. coli* XU363 to avoid changing the bacterial background.

Yeast strains and culture

The estradiol-inducible *ADH1* overexpression strain SY1144 is isogenic to diploid strain Y15090 (*MATa/α* [*HAP1-NatMX-ACT1pr-Z3EV-ENO2term*]/*HAP1 ura3 0/URA3* [*can1 ::STE2pr-SpHIS5*]/*CAN1 his3 1/his3 1 lyp1 /LYP1*)⁶⁵. Estradiol supplementation of the media causes translocation of a constitutively expressed Z₃EV artificial transcriptional activator into the nucleus. Z₃EV activates the expression of the *ADH1* gene, which was engineered to contain six Z₃EV binding sites in the promoter⁶⁵. Yeast strains were grown in Synthetic Complete (SC) media with 2% glucose for the chronological lifespan and western blotting assays. To induce *ADH1* expression, β-estradiol (dissolved in DMSO) was added to the liquid cultures at a final concentration of 6.25 or 100nM. All liquid cultures and agar plates were grown at 30°C.

METHOD DETAILS

C. elegans lifespan assays

Gravid worms of the strains of interest were bleached and the embryos rocked at 20°C for 18 hours to synchronize the hatchlings. After estimating the concentration of hatchlings by counting the number of hatchlings in 5x 5µl drops, around 200 hatchlings were seeded on NGM + 1mM IPTG + 25µg/mL carbenicillin plates (RNAi plates) seeded with *E. coli* strain XU363 carrying an empty L4440 plasmid (control). To initiate the lifespan assays, 30–40 young-adult worms were picked onto 6cm RNAi plates supplemented with 100µg/mL FUdR (RPI, United States) and seeded with *E. coli* XU363 carrying the L4440 control plasmid (EV) or a dsRNA-producing plasmid. For RNAi against *lgg-1*, knockdown was confirmed by western blotting (Figure S1E). When stated, cyanamide (1mM) or chloroquine (1mM) were added to plates right before transferring the young adults.

Aging experiments in the absence of FUdR (Figures S2 and S3C) were performed as described above but omitting the FUdR. Once worms reached adulthood, they were moved every day to fresh NGM plates seeded with *E. coli* XU363 L4440 (empty plasmid) until progenies were no longer produced.

For lifespan assays on glycerol, glycerol was added to the molten agar at a final concentration of 0.04% or 0.4%. Hatchlings were seeded on NGM plates without glycerol. Once worms reached the L4 stage, they were moved to glycerol containing-NGM plates seeded with OP50 and 50µM FUdR as previously described⁶⁶. Survival was scored daily or every other day. Worms were scored as dead if they did not respond to prodding with a platinum pick. Animals that escaped or died by bursting through the vulva were censored. Results were analyzed on SPSS using the Kaplan-Meier estimate with log rank test comparison across different strata. Figures were made using GraphPad Prism.

QUANTIFICATION AND STATISTICAL ANALYSIS

Data were considered statistically significant when $p < 0.05$ by Kaplan-Meier estimator with log rank test comparison across different strata (for aging experiments), unpaired Student's t-test or one-way and two-way ANOVA (for non-aging experiments) as indicated in the Figure, Figure legends or experimental methods. Asterisks denote corresponding statistical significance: ns = not significant, * $p < 0.05$, ** $p < 0.01$, *** $p < 0.001$, **** $p < 0.0001$. For aging experiments all p-values are reported in Data S1. Individual data points are presented where relevant, in addition to the mean and standard error of the mean (SEM) denoted by the error bars. The number of biological replicates for each experiment is stated in the legend of every figure or in the corresponding supplementary tables. In the figure legends or supplementary tables, N refers to the number of animals and n refers to the number of biological replicates. All statistical analyses were performed on SPSS (for aging experiments) or GraphPad Prism (for non-aging experiments).

Yeast lifespan assays

For yeast chronological lifespan assays (CLS), 10 mL of Synthetic Complete (SC) media with 2% glucose was inoculated with 100 µl of overnight culture and incubated on a roller

drum (TC-7, New Brunswick Scientific) in glass tubes with metal caps allowing for gas exchange. After 72 hours, the first measurement of colony forming units (CFUs) on YPD agar plates was made and this was treated as day 1 for the experiment (100% starting viability), to which all the other CFU data was normalized. Measurements were taken every 2 days as previously described^{67,68}. Briefly, at each time point, 20 μ l of the cell suspension were removed from each tube and 10-fold serially diluted three times with sterile water. Next, 2.5 μ l aliquots of each dilution were spotted onto a YPD plate. After 16 hours, images of the spots were taken under a Nikon Eclipse E400 brightfield microscope at 30x magnification. Microcolonies within the spots were automatically counted from the digital images using OrganoSeg⁶⁹, with the parameters adjusted for yeast colony counting⁶⁵. After accounting for the dilution factor, colony numbers from each day were divided by the number of colonies from the first time point (day 1) to calculate the viability score. Mean lifespan (in days) and the 95% confidence intervals were calculated using OASIS 2⁶⁹.

RT-qPCR

Worms were grown and synchronized as described in “Lifespan assays”. Approximately 1,500 synchronized L1 worms were seeded per 10cm RNAi plates containing control *E. coli* XU363. Once they reached the young adult stage, worms were transferred to RNAi plates containing 100 μ g/mL FUDR. At day 8 of adulthood, the animals were harvested using a mesh to remove the dead eggs, and worms were flash frozen in liquid nitrogen and preserved at -80°C until processing.

RNA extraction was performed on frozen worms using TRI Reagent (MRC, United States) as described by the manufacturer. The purity and concentration of the RNA samples were determined using a NanoDrop. 3 μ g of RNA were then used to synthesize 20 μ L of complementary DNA (cDNA).

Quantitative PCR was finally carried out by running a mixture of cDNA, SYBR green and primers for the genes of interest (Table S1) in a real time PCR thermal cycler (Biorad, United States). Fold changes were calculated using the Pfaffl method⁷¹ and statistical significance compared to the WT control was calculated using an unpaired Student’s t-test.

C. elegans western blotting

Worms were grown and synchronized as described in “Lifespan assays”. Approximately 2,000 synchronized L1 worms were seeded onto 10cm RNAi plates containing *E. coli* XU363 control. After growing the worms to day 1 adults, half the worms were transferred to RNAi plates containing 20mM chloroquine (Sigma, United States) while the other half of the worms (controls) were harvested, meshed to remove any laid eggs, and then flash frozen in liquid nitrogen. After 8 hours of treatment with chloroquine (CQ), CQ-treated animals were harvested, meshed, and flash frozen in liquid nitrogen.

RIPA buffer (Cold Spring Harbor protocols) was added to 100 μ L of packed worm pellets which were subsequently sonicated at 40% amplitude for 10 secs, a total of 5 times (keeping them on ice in between cycles). Protein content in the lysate was estimated using a Bradford assay (Thermo Scientific, United States), and lysates were then stored at -20°C after adding protein loading buffer. From each lysate, 30 μ g of protein were loaded and resolved in a

4–12% Bis-Tris precast gel (Thermo Scientific, United States, Cat #: NP0322BOX) and then transferred to a nitrocellulose membrane. The membrane was blocked using Intercept (PBS) Blocking Buffer (Li-cor, United States) for 4 hours at room temperature, followed by an overnight incubation in 1:250 of our previously published anti-LGG-1⁷² or in 1:5,000 anti-tubulin (DSHB, United States) primary antibodies. The next day, after washing, the membranes were incubated for an hour in the secondary antibody, Alexa Fluor® 800cw anti-rabbit (Li-cor, United States) or IRDye 800cw anti-mouse (Li-cor, United States). The proteins were visualized using a Li-cor Odyssey imaging system (Li-cor, United States) and the bands were quantified using densitometry analysis on ImageJ. Statistical significance compared to the WT and/or untreated control was calculated using an unpaired Student's t-test.

Yeast western blotting

Western blots for yeast proteins were performed as previously described⁷³. Cells were pelleted and stored at -80°C . To extract protein, cells were thawed on ice and resuspended in 0.5mL 20% trichloroacetic acid (TCA) at 4°C and then vortexed with glass beads 4 times for 30 seconds with 15 second rests on ice in between. Cell lysates were transferred to new microcentrifuge tubes. The beads were washed twice with 0.5mL 5% TCA at 4°C and the washes combined with the lysates, then centrifuged at 3,000 rpm for 10 minutes. Supernatants were discarded and the crude protein pellets were resuspended in 200 μL of sample buffer (50 mM Tris HCl, pH 6.8, 2% SDS, 10% glycerol, 0.1% bromophenol blue, 5% 2-mercaptoethanol). After resuspension, 50 μL of 2M Tris base was added and proteins were boiled for 5 minutes at 100°C . Samples (20 μL) were run on a 10% SDS polyacrylamide gel, then transferred onto PVDF membranes using a Biorad semi-dry transfer apparatus at 25 volts for 60 minutes. Membranes were blocked overnight with 5% non-fat milk in TBST at 4°C . Membranes were then incubated with either anti-alcohol dehydrogenase antibody (Rockland Immunochemicals, 200–4143-0100) at 1:1,000 or anti-alpha-tubulin antibody (Invitrogen, MA1–80017) at 1:5,000 in blocking buffer for 1 hour at room temperature. Membranes were washed in TBST once for 10 minutes followed by 3 washes for 5 minutes each. Membranes were then incubated in a secondary antibody, either HRP-conjugated anti-rabbit IgG (Promega Corporation, W4018) or HRP-conjugated anti-rat IgG (Abcam, ab6734) for 1 hour at room temperature. The membrane was washed again and then soaked for 5 minutes in HRP peroxidase substrate (Millipore, WBKLS0500), followed by a 1-minute soak in luminol (Millipore, WBKLS0500). Proteins were visualized using an Amersham ImageQuant 800 (Cytiva Life Sciences, 29399481) and the resulting bands were quantified using densitometry analysis on ImageJ. Statistical significance comparing Adh1 levels in CR relative to the non-restricted (NR) condition was determined by two-way ANOVA. Significance of estradiol induced Adh1 overexpression was determined by one-way ANOVA.

For caloric restriction, yeast cells were grown in Synthetic Complete (SC) media with 0.5% glucose. For no restriction (NR), they were grown in SC media containing 2% glucose. For Adh1 overexpression, beta-estradiol dissolved in DMSO was added to the SC NR media at the time of inoculation of yeast cells in concentrations of 0nM, 6.25nM and 100nM.

Immunostaining

Whole-body immunostaining against LGG-1 was performed as recently reported⁹³. Briefly, adult worms were treated with mock or chloroquine as described above and then fixed in 60% isopropanol. They were then immobilized on slides using a polyacrylamide gel where they were treated with β -mercaptoethanol and collagenase. Worms were then incubated in a blocking solution before being incubated in anti-LGG-1 antibody (1:250) overnight at 4°C. Worms were then washed and incubated in a goat anti-rabbit antibody (1:500) (Invitrogen, United States) at room temperature for 2 hours. Images were taken using a Leica spinning disk confocal microscope (Leica, Germany) and analyzed using ImageJ.

Allyl alcohol survival assay

Worms were grown and synchronized as described in “Lifespan assays”. Fifty day-1 adults were transferred to RNAi plates supplemented with 0.3% Allyl Alcohol (Sigma, United States). Worms were scored 4 hours post-treatment; animals not responding to prodding with a platinum pick were scored as dead. Statistical significance relative to the appropriate control was calculated using an unpaired Student’s t-test.

Fluorescent imaging

Worms were grown and synchronized as described in “Lifespan assays”. On day 1 of adulthood, ~100 worms were harvested and immobilized with 100mg/mL levamisole. Worms were then mounted on agar pads and imaged using a Leica spinning disk confocal microscope (Leica, Germany) at 60x magnification (numerical aperture: 1.4). The *daf-22P::PLIN1::GFP* was excited and visualized with a CSU-488 laser (emission filter 540 nm) and the *adh-1P::ADH-1::wrmScarlet::adh-13'UTR* was excited and visualized with a CSU-561 laser (emission filter 600 nm). We also imaged the *PLIN1::GFP;adh-1::WrmScarlet* strains in the blue channel (CSU-405 laser; emission filter 488 nm) to ensure that the signal observed in the other channels was not due to autofluorescence from the gut granules (Figure S4C). Images were analyzed using ImageJ. Statistical significance relative to the appropriate control was calculated using an unpaired Student’s t-test.

Glycerol measurement

Glycerol quantification was performed as previously described with some modifications⁷⁴. Worms were grown and synchronized as described in “Lifespan assays”. On day 1 (young) or 8 (aged) of adulthood, ~2,000 worms were harvested, flash-frozen in liquid nitrogen and stored at -80°C. Day 8 was picked because it is the last day that worms can be harvested without including a large number of dead animals in the samples. Additionally, by day 8, the worms already show significant signs of aging including damaged tissues, tubular lysosomes, atrophied intestine, and loss of self-fertility. To prepare worm lysates, 85 μ L of water was added to the frozen pellets of worms which were then sonicated for 10 seconds 5 times, keeping them for 2 minutes on ice between each sonication pulse. Samples were then centrifuged at 18,600g for 5 minutes at 4°C. Part of the supernatant was kept for protein quantification using a BCA assay, while the rest was deproteinized using trichloroacetic acid (TCA) and then neutralized following the manufacturer’s instructions

(AAT Bioquest, United States). The neutralization solution (AAT Bioquest, United States) was added to the samples until the pH was between 6.7–7.5. Glycerol was then measured in the deproteinized samples using a commercial kit following the manufacturer's protocol (R-Biopharm, Germany, Cat #: NC9662370). The measured amount of glycerol was then normalized to the corresponding sample's amount of protein, and to a standard glycerol curve per manufacturer instructions. Statistical significance relative to the appropriate control was calculated using an unpaired Student's t-test.

For glycerol measurement of HLH-30^{OE} animals, the same protocol was followed except L1 worms were grown on *E. coli* XU363 carrying L4440 + GFP plasmids before being switched to *E. coli* XU363 carrying L4440 (empty plasmid) at the L4 stage for 24 hours. The worms were then harvested as described above. This approach allowed us to perform an acute overexpression of HLH-30.

Locomotor endurance assay

Approximately twenty-four 12-days old worms were picked into individual wells of 24-well RNAi plates. Worms were allowed to adapt to the well for ~1h. Wells were then flushed one at a time with S-buffer and one-minute videos were taken using an Olympus SZX7 microscope fitted with an Olympus U-CMAD3 camera. Videos were then analyzed using the wrMTrack plugin on ImageJ⁷⁵. Statistical significance relative to the appropriate control was calculated using an unpaired Student's t-test.

Egg laying assay

As soon as the N2 and GMW20 (ADH-1^{OE}) worms reached the adult stage, single worms were picked into ten individual 6cc RNAi plates seeded with *E. coli* XU363 bacteria. Each of the ten worms was moved to fresh individual RNAi plates every 12h until reproduction ceased. The progenies laid during each 12h-period were allowed to develop until the L3-L4 stage at 20°C, and then counted. Statistical significance relative to the appropriate control was calculated using an unpaired Student's t-test.

Glycerol choice assay

Eight 10µL spots of *E. coli* XU363 were seeded on 10cc RNAi plates equidistant from the plate-center and from each other. Alternating between the spots, glycerol was added to 4 of the *E. coli* XU363 spots. In parallel 1-day old worms were harvested, washed with S-buffer, and the concentration of worms in the suspension was estimated by counting worms in five 5µl drops. Worms were concentrated to five worms per microliter by centrifugation. To start the assay, approximately 200 synchronized adult worms (40µl) were seeded in the center of the plate. Plates were incubated at 20°C. After 3h, 6h, 12h and 24h, the number of worms on each spot was counted. Statistical significance was calculated using an unpaired Student's t-test.

QUANTIFICATION AND STATISTICAL ANALYSIS

Data were considered statistically significant when $p < 0.05$ by Kaplan-Meier estimator with log rank test comparison across different strata (for aging experiments), unpaired Student's

t-test or one-way and two-way ANOVA (for non-aging experiments) as indicated in the Figure, Figure legends or experimental methods. Asterisks denote corresponding statistical significance: ns = not significant, * $p < 0.05$, ** $p < 0.01$, *** $p < 0.001$, **** $p < 0.0001$. For aging experiments all p-values are reported in Data S1. Individual data points are presented where relevant, in addition to the mean and standard error of the mean (SEM) denoted by the error bars. The number of biological replicates for each experiment is stated in the legend of every figure or in the corresponding supplementary tables. In the figure legends or supplementary tables, N refers to the number of animals and n refers to the number of biological replicates. All statistical analyses were performed on SPSS (for aging experiments) or GraphPad Prism (for non-aging experiments).

RESOURCE AVAILABILITY

Lead contact

Further information and requests for resources and reagents should be directed to and will be fulfilled by the lead contact, Dr. Eyleen O'Rourke (ejourourke@virginia.edu).

Materials availability

C. elegans strains generated in this study will be made publicly available through the Caenorhabditis Genetics Center (CGC) after the first personal request.

Data and code availability

- All data generated in this study are available in the main paper, supplemental information and supplemental excel file. This paper also analyzes existing, publicly available datasets: the accession numbers for the datasets are listed in the key resources table.
- This paper does not report original code.
- Any additional information required to reanalyze the data reported in this paper is available from the lead contact upon request.

Supplementary Material

Refer to Web version on PubMed Central for supplementary material.

Acknowledgements

We thank Drs. Monica Driscoll and Xun Huang for sharing the XD3971 LD reporter strain. We thank Dr. Felipe Cabreiro for providing advice on the glycerol-supplementation lifespan assay. We thank Dr. Kevin Janes for comments on the manuscript. We thank Nella Solodukhina for helping manage the lab and preparing reagents. Yeast strains were provided by Calico Labs and Charles Boone's lab at the University of Toronto. AG was supported by a dissertation-year fellowship from the Society of Fellows (UVA) and a Harrison Family Jefferson Fellowship from the Jefferson Scholars Foundation. EEH was supported by the Medical Scientist Training Program (MSTP) training grant T32GM007267, the Cell and Molecular Biology (CMB) training grant T32GM008136, and an individual National Research Service Award (F30AG067760) from the National Institutes of Health (NIH). JSS is supported by NIH grants RO1GM075240 and RO1GM127394. EJO is supported by a Biomedical Scholars award from the Pew Charitable Trusts, an award from the Jeffress Trust, and grants from the NIH (DK087928) and W.M. Keck Foundation. Finally, we would like to acknowledge the CGC, which is funded by NIH Office of Research Infrastructure Programs (P40 OD010440), for providing *C. elegans* strains.

References

1. Lapierre LR, De Magalhaes Filho CD, McQuary PR, Chu C-C, Visvikis O, Chang JT, Gelino S, Ong B, Davis AE, Irazoqui JE, et al. (2013). The TFEB orthologue HLH-30 regulates autophagy and modulates longevity in *Caenorhabditis elegans*. *Nat. Commun* 4, 2267. [PubMed: 23925298]
2. Mony VK, Drangowska-Way A, Albert R, Harrison E, Ghaddar A, Horak MK, Ke W, O'Rourke EJ, (2021). Context-specific regulation of lysosomal lipolysis through network-level diverting of transcription factor interactions. *Proc Natl Acad Sci U S A* 118(41):e210483211
3. O'Rourke EJ, and Ruvkun G (2013). MXL-3 and HLH-30 transcriptionally link lipolysis and autophagy to nutrient availability. *Nat. Cell Biol* 15, 668–676. [PubMed: 23604316]
4. Zhang W, Li X, Wang S, Chen Y, and Liu H (2020). Regulation of TFEB activity and its potential as a therapeutic target against kidney diseases. *Cell Death Discov* 6, 32. [PubMed: 32377395]
5. Zhang X, Chen W, Gao Q, Yang J, Yan X, Zhao H, Su L, Yang M, Gao C, Yao Y, et al. (2019). Rapamycin directly activates lysosomal mucolipin TRP channels independent of mTOR. *PLoS Biol* 17, e3000252. [PubMed: 31112550]
6. Polito VA, Li H, Martini-Stoica H, Wang B, Yang L, Xu Y, Swartzlander DB, Palmieri M, di Ronza A, Lee VM-Y, et al. (2014). Selective clearance of aberrant tau proteins and rescue of neurotoxicity by transcription factor EB. *EMBO Mol. Med* 6, 1142–1160. [PubMed: 25069841]
7. Decressac M, Mattsson B, Weikop P, Lundblad M, Jakobsson J, and Björklund A (2013). TFEB-mediated autophagy rescues midbrain dopamine neurons from α -synuclein toxicity. *Proc Natl Acad Sci USA* 110, E1817–26. [PubMed: 23610405]
8. Pastore N, Ballabio A, and Brunetti-Pierrri N (2013). Autophagy master regulator TFEB induces clearance of toxic SERPINA1/ α -1-antitrypsin polymers. *Autophagy* 9, 1094–1096. [PubMed: 23584152]
9. Settembre C, Di Malta C, Polito VA, Garcia Arencibia M, Vetrini F, Erdin S, Erdin SU, Huynh T, Medina D, Colella P, et al. (2011). TFEB links autophagy to lysosomal biogenesis. *Science* 332, 1429–1433. [PubMed: 21617040]
10. Jia K, and Levine B (2007). Autophagy is required for dietary restriction-mediated life span extension in *C. elegans*. *Autophagy* 3, 597–599. [PubMed: 17912023]
11. Hansen M, Chandra A, Mitic LL, Onken B, Driscoll M, and Kenyon C (2008). A role for autophagy in the extension of lifespan by dietary restriction in *C. elegans*. *PLoS Genet* 4, e24. [PubMed: 18282106]
12. Hansen M, Rubinsztein DC, and Walker DW (2018). Autophagy as a promoter of longevity: insights from model organisms. *Nat. Rev. Mol. Cell Biol* 19, 579–593. [PubMed: 30006559]
13. Cuervo AM (2008). Autophagy and aging: keeping that old broom working. *Trends Genet* 24, 604–612. [PubMed: 18992957]
14. Choi AMK, Ryter SW, and Levine B (2013). Autophagy in human health and disease. *N. Engl. J. Med* 368, 1845–1846.
15. Grove CA, De Masi F, Barrasa MI, Newburger DE, Alkema MJ, Bulyk ML, and Walhout AJM (2009). A multiparameter network reveals extensive divergence between *C. elegans* bHLH transcription factors. *Cell* 138, 314–327. [PubMed: 19632181]
16. Harvald EB, Sprenger RR, Dall KB, Ejsing CS, Nielsen R, Mandrup S, Murillo AB, Larance M, Gartner A, Lamond AI, et al. (2017). Multi-omics Analyses of Starvation Responses Reveal a Central Role for Lipoprotein Metabolism in Acute Starvation Survival in *C. elegans*. *Cell Syst* 5, 38–52.e4. [PubMed: 28734827]
17. ENCODE Project Consortium (2012). An integrated encyclopedia of DNA elements in the human genome. *Nature* 489, 57–74. [PubMed: 22955616]
18. Celniker SE, Dillon LAL, Gerstein MB, Gunsalus KC, Henikoff S, Karpen GH, Kellis M, Lai EC, Lieb JD, MacAlpine DM, et al. (2009). Unlocking the secrets of the genome. *Nature* 459, 927–930. [PubMed: 19536255]
19. Gao AW, Smith RL, van Weeghel M, Kamble R, Janssens GE, and Houtkooper RH (2018). Identification of key pathways and metabolic fingerprints of longevity in *C. elegans*. *Exp. Gerontol* 113, 128–140. [PubMed: 30300667]

20. Murphy CT, McCarroll SA, Bargmann CI, Fraser A, Kamath RS, Ahringer J, Li H, and Kenyon C (2003). Genes that act downstream of DAF-16 to influence the lifespan of *Caenorhabditis elegans*. *Nature* 424, 277–283. [PubMed: 12845331]
21. Tissenbaum HA, and Ruvkun G (1998). An insulin-like signaling pathway affects both longevity and reproduction in *Caenorhabditis elegans*. *Genetics* 148, 703–717. [PubMed: 9504918]
22. Good TP, and Tatar M (2001). Age-specific mortality and reproduction respond to adult dietary restriction in *Drosophila melanogaster*. *J. Insect Physiol* 47, 1467–1473. [PubMed: 12770153]
23. Widholm JM, and Kishinami I (1988). Allyl Alcohol Selection for Lower Alcohol Dehydrogenase Activity in *Nicotiana plumbaginifolia* Cultured Cells. *Plant Physiol* 86, 266–269. [PubMed: 16665878]
24. Plapp BV, Lee AT-I, Khanna A, and Pryor JM (2013). Bradykinetic alcohol dehydrogenases make yeast fitter for growth in the presence of allyl alcohol. *Chem. Biol. Interact* 202, 104–110. [PubMed: 23200945]
25. Toennes SW, Schmidt K, Fandiño AS, and Kauert GF (2002). A fatal human intoxication with the herbicide allyl alcohol (2-propen-1-ol). *J. Anal. Toxicol* 26, 55–57. [PubMed: 11888018]
26. Serafini-Cessi F (1972). Conversion of allyl alcohol into acrolein by rat liver. *Biochem. J* 128, 1103–1107. [PubMed: 4404964]
27. Ghaddar A, Armingol E, Huynh C, Gevirtzman L, Lewis NE, Waterston R, and O'Rourke EJ (2022). Whole-body gene expression atlas of an adult metazoan. *BioRxiv*
28. El Mouridi S, Lecroisey C, Tardy P, Mercier M, Leclercq-Blondel A, Zariohi N, Boulin T (2017) Reliable CRISPR/Cas9 Genome Engineering in *Caenorhabditis elegans* Using a Single Efficient sgRNA and an Easily Recognizable Phenotype. *G3 (Bethesda)* 7, 1429–1437. [PubMed: 28280211]
29. Heick HM, Willemot J, and Begin-Heick N (1969). The subcellular localization of alcohol dehydrogenase activity in baker's yeast. *Biochim. Biophys. Acta* 191, 493–501. [PubMed: 4312202]
30. de Smidt O, du Preez JC, and Albertyn J (2008). The alcohol dehydrogenases of *Saccharomyces cerevisiae*: a comprehensive review. *FEMS Yeast Res* 8, 967–978. [PubMed: 18479436]
31. Liu Z, Li X, Ge Q, Ding M, and Huang X (2014). A lipid droplet-associated GFP reporter-based screen identifies new fat storage regulators in *C. elegans*. *J. Genet. Genomics* 41, 305–313. [PubMed: 24894357]
32. Lee S-J, Murphy CT, and Kenyon C (2009). Glucose shortens the life span of *C. elegans* by downregulating DAF-16/FOXO activity and aquaporin gene expression. *Cell Metab* 10, 379–391. [PubMed: 19883616]
33. Edwards C, Canfield J, Copes N, Brito A, Rehan M, Lipps D, Brunquell J, Westerheide SD, and Bradshaw PC (2015). Mechanisms of amino acid-mediated lifespan extension in *Caenorhabditis elegans*. *BMC Genet* 16, 8. [PubMed: 25643626]
34. Shirota FN, Stevens-Johnk JM, DeMaster EG, and Nagasawa HT (1997). Novel prodrugs of cyanamide that inhibit aldehyde dehydrogenase in vivo. *J. Med. Chem* 40, 1870–1875. [PubMed: 9191964]
35. Loomis CW, and Brien JF (1983). Inhibition of hepatic aldehyde dehydrogenases in the rat by calcium carbimide (calcium cyanamide). *Can. J. Physiol. Pharmacol* 61, 1025–1034. [PubMed: 6640426]
36. Grzelak A, Macierzy ska E, and Bartosz G (2006). Accumulation of oxidative damage during replicative aging of the yeast *Saccharomyces cerevisiae*. *Exp. Gerontol* 41, 813–818. [PubMed: 16891074]
37. Medina DL, Fraldi A, Bouche V, Annunziata F, Mansueto G, Spampanato C, Puri C, Pignata A, Martina JA, Sardiello M, et al. (2011). Transcriptional activation of lysosomal exocytosis promotes cellular clearance. *Dev. Cell* 21, 421–430. [PubMed: 21889421]
38. Rocznik-Ferguson A, Petit CS, Froehlich F, Qian S, Ky J, Angarola B, Walther TC, and Ferguson SM (2012). The transcription factor TFE3 links mTORC1 signaling to transcriptional control of lysosome homeostasis. *Sci. Signal* 5, ra42. [PubMed: 22692423]

39. Palmieri M, Impey S, Kang H, di Ronza A, Pelz C, Sardiello M, and Ballabio A (2011). Characterization of the CLEAR network reveals an integrated control of cellular clearance pathways. *Hum. Mol. Genet* 20, 3852–3866. [PubMed: 21752829]
40. Sardiello M, and Ballabio A (2009). Lysosomal enhancement: a CLEAR answer to cellular degradative needs. *Cell Cycle* 8, 4021–4022. [PubMed: 19949301]
41. Chen H-D, Kao C-Y, Liu B-Y, Huang S-W, Kuo C-J, Ruan J-W, Lin Y-H, Huang C-R, Chen Y-H, Wang H-D, et al. (2017). HLH-30/TFEB-mediated autophagy functions in a cell-autonomous manner for epithelium intrinsic cellular defense against bacterial pore-forming toxin in *C. elegans*. *Autophagy* 13, 371–385. [PubMed: 27875098]
42. Pan B, Zhang H, Cui T, and Wang X (2017). TFEB activation protects against cardiac proteotoxicity via increasing autophagic flux. *J. Mol. Cell. Cardiol* 113, 51–62. [PubMed: 28993153]
43. Visvikis O, Ihuegbu N, Labed SA, Luhachack LG, Alves A-MF, Wollenberg AC, Stuart LM, Stormo GD, and Irazoqui JE (2014). Innate host defense requires TFEB-mediated transcription of cytoprotective and antimicrobial genes. *Immunity* 40, 896–909. [PubMed: 24882217]
44. Chen M, Dai Y, Liu S, Fan Y, Ding Z, and Li D (2021). TFEB biology and agonists at a glance. *Cells* 10.
45. Gerisch B, Tharyan RG, Mak J, Denzel SI, Popkes-van Oepen T, Henn N, and Antebi A (2020). HLH-30/TFEB Is a Master Regulator of Reproductive Quiescence. *Dev. Cell* 53, 316–329.e5. [PubMed: 32302543]
46. Palmisano NJ, and Meléndez A (2019). Autophagy in *C. elegans* development. *Dev. Biol* 447, 103–125. [PubMed: 29709599]
47. Meléndez A, and Neufeld TP (2008). The cell biology of autophagy in metazoans: a developing story. *Development* 135, 2347–2360. [PubMed: 18567846]
48. Lapierre LR, Silvestrini MJ, Nuñez L, Ames K, Wong S, Le TT, Hansen M, and Meléndez A (2013). Autophagy genes are required for normal lipid levels in *C. elegans*. *Autophagy* 9, 278–286. [PubMed: 23321914]
49. Kocaturk NM, and Gozuacik D (2018). Crosstalk Between Mammalian Autophagy and the Ubiquitin-Proteasome System. *Front. Cell Dev. Biol* 6, 128. [PubMed: 30333975]
50. Saftig P, and Puertollano R (2021). How Lysosomes Sense, Integrate, and Cope with Stress. *Trends Biochem. Sci* 46, 97–112. [PubMed: 33012625]
51. Hashimoto Y, Ookuma S, and Nishida E (2009). Lifespan extension by suppression of autophagy genes in *Caenorhabditis elegans*. *Genes Cells* 14, 717–726. [PubMed: 19469880]
52. Doepfner TR, Coman C, Burdusel D, Ancuta D-L, Brockmeier U, Pirici DN, Yaoyun K, Hermann DM, and Popa-Wagner A (2022). Long-term treatment with chloroquine increases lifespan in middle-aged male mice possibly via autophagy modulation, proteasome inhibition and glycogen metabolism. *Aging (Albany NY)* 14, 4195–4210. [PubMed: 35609021]
53. Agarwal S, and Sohal RS (1994). Aging and protein oxidative damage. *Mech. Ageing Dev* 75, 11–19. [PubMed: 9128750]
54. Pozzato G, Moretti M, Franzin F, Crocè LS, Lacchin T, Benedetti G, Sablich R, Stebel M, and Campanacci L (1995). Ethanol metabolism and aging: the role of “first pass metabolism” and gastric alcohol dehydrogenase activity. *J. Gerontol. A Biol. Sci. Med. Sci* 50, B135–41. [PubMed: 7743392]
55. Petrosino JM, Longenecker JZ, Ramkumar S, Xu X, Dorn LE, Bratasz A, Yu L, Maurya S, Tolstikov V, Bussberg V, et al. (2021). Paracardial fat remodeling affects systemic metabolism through alcohol dehydrogenase 1. *J. Clin. Invest* 131.
56. Seitz HK, Meydani M, Ferschke I, Simanowski UA, Boesche J, Bogusz M, Hoepker WW, Blumberg JB, and Russell RM (1989). Effect of aging on in vivo and in vitro ethanol metabolism and its toxicity in F344 rats. *Gastroenterology* 97, 446–456. [PubMed: 2744358]
57. Kayo T, Allison DB, Weindruch R, and Prolla TA (2001). Influences of aging and caloric restriction on the transcriptional profile of skeletal muscle from rhesus monkeys. *Proc Natl Acad Sci USA* 98, 5093–5098. [PubMed: 11309484]

58. Plank M, Wuttke D, van Dam S, Clarke SA, and de Magalhães JP (2012). A meta-analysis of caloric restriction gene expression profiles to infer common signatures and regulatory mechanisms. *Mol. Biosyst* 8, 1339–1349. [PubMed: 22327899]
59. Tyshkovskiy A, Bozaykut P, Borodinova AA, Gerashchenko MV, Ables GP, Garratt M, Khaitovich P, Clish CB, Miller RA, and Gladyshev VN (2019). Identification and Application of Gene Expression Signatures Associated with Lifespan Extension. *Cell Metab* 30, 573–593.e8. [PubMed: 31353263]
60. Balak KJ, Keith RH, and Felder MR (1982). Genetic and developmental regulation of mouse liver alcohol dehydrogenase. *J. Biol. Chem* 257, 15000–15007. [PubMed: 6816803]
61. Yuan R, Meng Q, Nautiyal J, Flurkey K, Tsaih S-W, Krier R, Parker MG, Harrison DE, and Paigen B (2012). Genetic coregulation of age of female sexual maturation and lifespan through circulating IGF1 among inbred mouse strains. *Proc Natl Acad Sci USA* 109, 8224–8229. [PubMed: 22566614]
62. Wang Y, Zhang Y, Zhang X, Yang T, Liu C, and Wang P (2019). Alcohol Dehydrogenase 1B Suppresses β -Amyloid-Induced Neuron Apoptosis. *Front. Aging Neurosci* 11, 135. [PubMed: 31231206]
63. Guo KK, and Ren J (2006). Cardiac overexpression of alcohol dehydrogenase (ADH) alleviates aging-associated cardiomyocyte contractile dysfunction: role of intracellular Ca²⁺ cycling proteins. *Aging Cell* 5, 259–265. [PubMed: 16842498]
64. Xiao R, Chun L, Ronan EA, Friedman DI, Liu J, and Xu XZS (2015). RNAi Interrogation of Dietary Modulation of Development, Metabolism, Behavior, and Aging in *C. elegans*. *Cell Rep* 11, 1123–1133. [PubMed: 25959815]
65. Arita Y, Kim G, Li Z, Friesen H, Turco G, Wang RY, Climie D, Usaj M, Hotz M, Stoops EH, et al. (2021). A genome-scale yeast library with inducible expression of individual genes. *Mol. Syst. Biol* 17, e10207. [PubMed: 34096681]
66. Pryor R, Norvaisas P, Marinos G, Best L, Thingholm LB, Quintaneiro LM, De Haes W, Esser D, Waschina S, Lujan C., et al. (2019). Host-Microbe-Drug-Nutrient Screen Identifies Bacterial Effectors of Metformin Therapy. *Cell* 178(6):1299–1312.e29. doi: 10.1016/j.cell.2019.08.003. Epub 2019 Aug 29. [PubMed: 31474368]
67. Enriquez-Hesles E, Smith DL, Maqani N, Wierman MB, Sutcliffe MD, Fine RD, Kalita A, Santos SM, Muehlbauer MJ, Bain JR, et al. (2021). A cell-nonautonomous mechanism of yeast chronological aging regulated by caloric restriction and one-carbon metabolism. *J. Biol. Chem* 296, 100125. [PubMed: 33243834]
68. Wierman MB, Maqani N, Strickler E, Li M, and Smith JS (2017). Caloric restriction extends yeast chronological life span by optimizing the snf1 (AMPK) signaling pathway. *Mol. Cell. Biol* 37.
69. Borten MA, Bajikar SS, Sasaki N, Clevers H, and Janes KA (2018). Automated brightfield morphometry of 3D organoid populations by OrganoSeg. *Sci. Rep* 8, 5319. [PubMed: 29593296]
70. Han SK, Lee D, Lee H, Kim D, Son HG, Yang J-S, Lee S-JV, and Kim S (2016). OASIS 2: online application for survival analysis 2 with features for the analysis of maximal lifespan and healthspan in aging research. *Oncotarget* 7, 56147–56152. [PubMed: 27528229]
71. Pfaffl MW (2001). A new mathematical model for relative quantification in real-time RT-PCR. *Nucleic Acids Res* 29, e45. [PubMed: 11328886]
72. Ke W, Saba JA, Yao C-H, Hilzendege MA, Drangowska-Way A, Joshi C, Mony VK, Benjamin SB, Zhang S, Locasale J, et al. (2020). Dietary serine-microbiota interaction enhances chemotherapeutic toxicity without altering drug conversion. *Nat. Commun* 11, 2587. [PubMed: 32444616]
73. Hontz RD, Niederer RO, Johnson JM, and Smith JS (2009). Genetic identification of factors that modulate ribosomal DNA transcription in *Saccharomyces cerevisiae*. *Genetics* 182, 105–119. [PubMed: 19270272]
74. Burkewitz K, Choe KP, Lee EC-H, Deonarine A, and Strange K (2012). Characterization of the proteostasis roles of glycerol accumulation, protein degradation and protein synthesis during osmotic stress in *C. elegans*. *PLoS ONE* 7, e34153. [PubMed: 22470531]

75. Nussbaum-Krammer CI, Neto MF, Briellmann RM, Pedersen JS, and Morimoto RI (2015). Investigating the spreading and toxicity of prion-like proteins using the metazoan model organism *C. elegans*. *J. Vis. Exp* 52321. [PubMed: 25591151]
76. Armenise C, Lefebvre G, Carayol J, Bonnel S, Bolton J, Di Cara A, Gheldof N, Descombes P, Langin D, Saris WH., et al. (2017). Transcriptome profiling from adipose tissue during a low-calorie diet reveals predictors of weight and glycemic outcomes in obese, nondiabetic subjects. *Am J Clin Nutr* 106(3):736–746. doi: 10.3945/ajcn.117.156216. Epub 2017 Aug 9. [PubMed: 28793995]
77. Capel F, Viguerie N, Vega N, Dejean S, Arner P, Klimcakova E, Martinez JA, Saris WH, Holst C, Taylor M, et al. (2008). Contribution of energy restriction and macronutrient composition to changes in adipose tissue gene expression during dietary weight-loss programs in obese women. *J Clin Endocrinol Metab* 93(11):4315–22. doi: 10.1210/jc.2008-0814. Epub 2008 Sep 9. [PubMed: 18782868]
78. Tareen SHK., Kutmon M, de Kok TM, Mariman ECM, van Baak MA, Evelo CT, Adriaens ME, Arts ICW, (2020). Stratifying cellular metabolism during weight loss: an interplay of metabolism, metabolic flexibility and inflammation. *Sci Rep* 10(1):1651. doi: 10.1038/s41598-020-58358-z. [PubMed: 32015415]
79. Capel F, Klimčáková E, Viguerie N, Roussel B, Vítková M, Kováčiková M, Polák J, Kováčová Z, Galitzky J, Maoret JJ., et al. (2009). Macrophages and adipocytes in human obesity: adipose tissue gene expression and insulin sensitivity during calorie restriction and weight stabilization. *Diabetes* 58(7):1558–67. doi: 10.2337/db09-0033. Epub 2009 Apr 28. [PubMed: 19401422]
80. Mutch DM., Pers TH., Temanni MR, Pelloux V, Marquez-Quiñones A, Holst C, Martinez JA, Babalis D, van Baak MA, Handjieva-Darlenska T, et al. (2011). A distinct adipose tissue gene expression response to caloric restriction predicts 6-mo weight maintenance in obese subjects. *Am J Clin Nutr* 94(6):1399–409. doi: 10.3945/ajcn.110.006858. Epub 2011 Oct 26. [PubMed: 22030226]
81. Nookaew I, Svensson PA, Jacobson P, Jernås M, Taube M, Larsson I, Andersson-Assarsson JC, Sjöström L, Froguel P, Walley A, et al. (2013). Adipose tissue resting energy expenditure and expression of genes involved in mitochondrial function are higher in women than in men. *J Clin Endocrinol Metab* 98(2):E370–8. doi: 10.1210/jc.2012-2764. Epub 2012 Dec 21. [PubMed: 23264395]
82. Noyan H, El-Mounayri O, Isserlin R, Arab S, Momen A, Cheng HS, Wu J, Afroze T, Li RK, Fish JE, et al. (2015). Cardioprotective Signature of Short-Term Caloric Restriction. *PLoS One*, 10(6):e0130658. doi: 10.1371/journal.pone.0130658. [PubMed: 26098549]
83. Kim SS., Choi KM, Kim S, Park T, Cho IC, Lee JW, Lee CK (2016). Whole-transcriptome analysis of mouse adipose tissue in response to short-term caloric restriction. *Mol Genet Genomics*, 291(2):831–47. doi: 10.1007/s00438-015-1150-3. Epub 2015 Nov 25. [PubMed: 26606930]
84. Higami Y, Pugh TD, Page GP, Allison DB, Prola TA, Weindruch R, (2004). Adipose tissue energy metabolism: altered gene expression profile of mice subjected to long-term caloric restriction. *FASEB J* 18(2):415–7. doi: 10.1096/fj.03-0678fje. Epub 2003 Dec 19. [PubMed: 14688200]
85. Mitchell SJ., Madrigal-Matute J, Scheibye-Knudsen M, Fang E, Aon M, González-Reyes JA, Cortassa S, Kaushik S, Gonzalez-Freire M, Patel B, et al. (2016). Effects of Sex, Strain, and Energy Intake on Hallmarks of Aging in Mice. *Cell Metab* 23(6):1093–1112. doi: 10.1016/j.cmet.2016.05.027. [PubMed: 27304509]
86. Tsuchiya T, Dhahbi JM, Cui X, Mote PL, Bartke A, Spindler SR, (2004). Additive regulation of hepatic gene expression by dwarfism and caloric restriction. *Physiol Genomics*, 19;17(3):307–15. doi: 10.1152/physiolgenomics.00039.2004. [PubMed: 15039484]
87. Pohjanvirta R, Boutros PC, Moffat ID, Lindén J, Wendelin D, Okey AB, (2008). Genome-wide effects of acute progressive feed restriction in liver and white adipose tissue. *Toxicol Appl Pharmacol* 230(1):41–56. doi: 10.1016/j.taap.2008.02.002. Epub 2008 Feb 14. [PubMed: 18394668]
88. Hakvoort TB., Moerland PD., Frijters R., Sokolovi A., Labruyère WT., Vermeulen JL., Ver Loren van Themaat E, Breit TM., Wittink FR., van Kampen AH., et al. (2011). Interorgan coordination of the murine adaptive response to fasting. *J Biol Chem* 286(18):16332–43. doi: 10.1074/jbc.M110.216986. Epub 2011 Mar 10. [PubMed: 21393243]

89. Lanza IR., Zabielski P., Klaus KA., Morse DM., Heppelmann CJ., Bergen HR. 3rd, Dasari S., Walrand S, Short KR., Johnson ML., et al. (2012). Chronic caloric restriction preserves mitochondrial function in senescence without increasing mitochondrial biogenesis. *Cell Metab* 16(6):777–88. doi: 10.1016/j.cmet.2012.11.003. [PubMed: 23217257]
90. Jongbloed F, de Bruin RW, Pennings JL, Payán-Gómez C, van den Engel S, van Oostrom CT., de Bruin A., Hoeijmakers JH., van Steeg H., IJzermans JN., et al. (2014). Preoperative fasting protects against renal ischemia-reperfusion injury in aged and overweight mice. *PLoS One*, 9(6):e100853. doi: 10.1371/journal.pone.0100853. [PubMed: 24959849]
91. Someya S, Yamasoba T, Weindruch R, Prolla TA, Tanokura M, (2007). Caloric restriction suppresses apoptotic cell death in the mammalian cochlea and leads to prevention of presbycusis. *Neurobiol Aging* 28(10):1613–22. doi: 10.1016/j.neurobiolaging.2006.06.024. Epub 2006 Aug 4. [PubMed: 16890326]
92. Aon MA., Bernier M., Mitchell SJ., Di Germanio C., Mattison JA., Ehrlich MR., Colman RJ., Anderson RM., de Cabo R., (2020). Untangling Determinants of Enhanced Health and Lifespan through a Multi-omics Approach in Mice. *Cell Metab* 32(1):100–116.e4. doi: 10.1016/j.cmet.2020.04.018. Epub 2020 May 14. [PubMed: 32413334]
93. Ghaddar A, Ke W, O'Rourke E Immunostaining of intact *C. elegans* using polyacrylamide embedding. *STAR Protoc* 2023. doi:10.1016/j.xpro.2022.101956

eTOC blurb

Ghaddar, Mony *et al.* show that longevity caused by activation of the transcriptional activator of autophagy, TFEB/HLH-30, may not always require autophagy. Instead, they present the Alcohol-dehydrogenase Mediated anti-Aging Response (AMAR) as an HLH-30/TFEB-dependent, but more importantly, necessary and sufficient anti-aging effector acting across interventions and organisms.

Highlights:

- AMAR is required for longevity across anti-aging interventions
- AMAR is sufficient to promote longevity in *C. elegans* and yeast
- AMAR extends lifespan, at least in part, by metabolizing glycerol
- AMAR is activated in response to geroprotective interventions in mice and humans

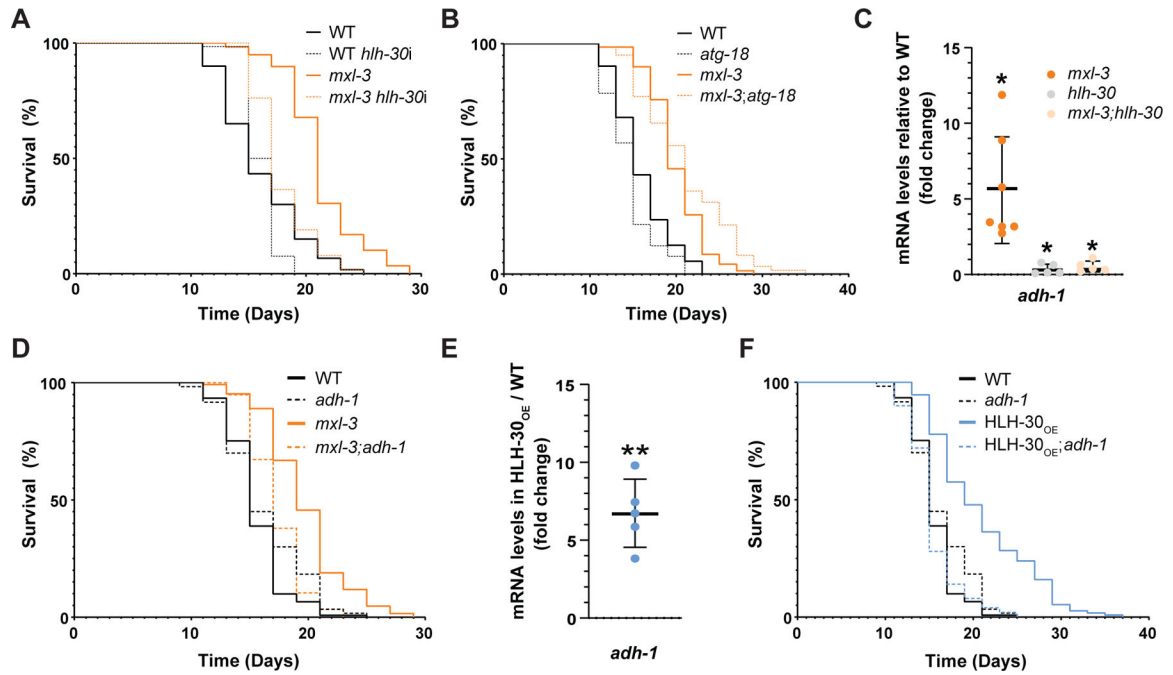


Figure 1. *adh-1* activation drives HLH-30-mediated longevity.

(A) The master regulator of autophagy and lysosomal biogenesis, TF *hlh-30/Tfeb*, is required for the longevity phenotype of the *mxl-3* *C. elegans* mutant (representative of 3 biological replicates; see Data S1A). (B) Loss-of-function mutation of the non-lethal autophagy gene *atg-18* does not suppress *mxl-3* longevity (representative of 3 biological replicates; see Data S1C). In addition, autophagy levels are not elevated at the transcriptional (Figure S1A), biochemical (Figure S1B), or cellular (Figure S1C) levels in the *mxl-3* mutant, and post-developmental RNAi against the lethal autophagy genes *bec-1* and *lgg-1* or full inhibition of lysosomal activity and autophagy with chloroquine do not suppress *mxl-3* longevity (Figure S1D-E). (C) As measured by RT-qPCR, *adh-1* transcript levels are elevated in the *mxl-3* mutant in an *hlh-30* dependent manner (n=5–7 biological replicates). See Table S1 for RT-qPCR primers. (D) The longevity of the *mxl-3* mutant is suppressed by loss-of-function mutation of *adh-1* (representative of three biological replicates; see Data S1D). (E) *adh-1* transcript levels are elevated in the HLH-30^{OE} animals (n=5 biological replicates). (F) Loss-of-function mutation of *adh-1* fully suppresses the extended lifespan of the HLH-30^{OE} animals (representative of 3 biological replicates; see Data S1D and Figure S2). (A-F) Error bars denote SEM. ns= not significant, *p<0.05, **p<0.01, ***p<0.001, ****p<0.0001; *hlh-30* = *hlh-30* RNAi. All experiments were performed using *E. coli* XU363 carrying L4440 (empty vector) or L4440 + the gene of interest.

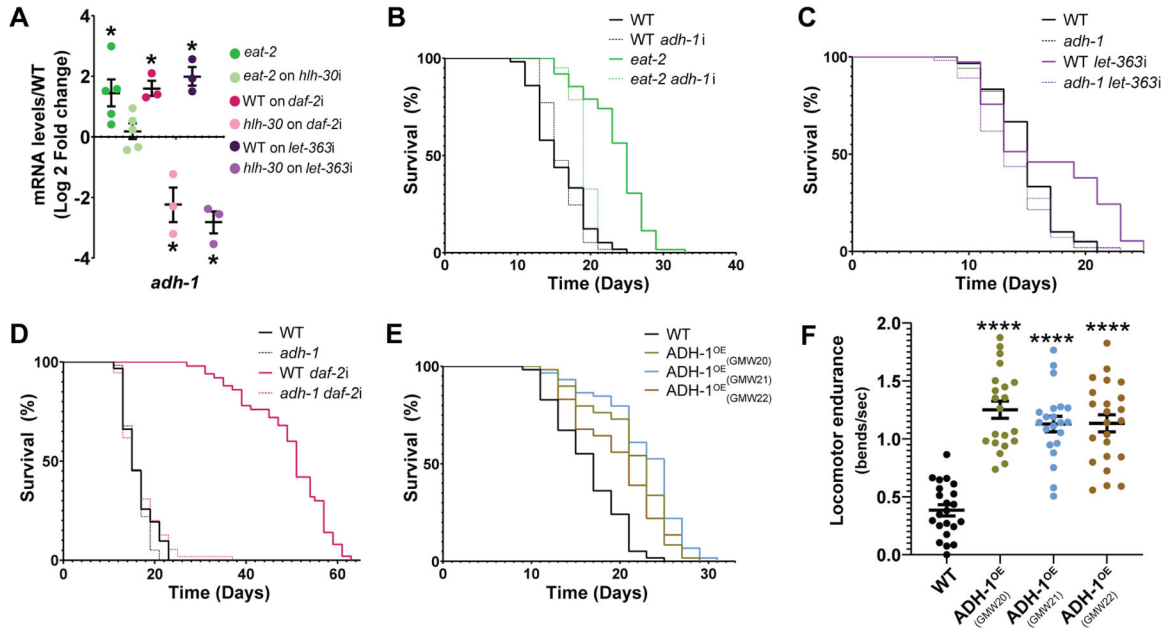


Figure 2. *adh-1* is necessary and sufficient to extend lifespan and healthspan.

(A) *adh-1* is induced in an *hlh-30*-dependent manner in the longevity models caloric restriction (*eat-2*), insulin insensitivity (*daf-2*), and mTOR inhibition (*let-363* RNAi) (n=3 to 5 biological replicates). See Table S1 for RT-qPCR primers. (B-D) In *C. elegans*, *adh-1* is required for longevity driven by (B) caloric restriction, (C) mTOR inhibition, and (D) deficient insulin-signaling (representative of three biological replicates; see Data S1F-H). (E) Overexpressing ADH-1 (ADH-1^{OE}) is sufficient to promote longevity in *C. elegans*. Survival curves for three independent overexpression lines (GWM20–22) are presented (representative of three biological replicates; see Data S1I). (F) ADH-1 promotes locomotor endurance as measured by thrashing in liquid medium in 12-days old ADH-1^{OE} and wild-type *C. elegans* (representative of three biological replicates; repeats in Data S1N). Also see Figure S3 for further characterization of *C. elegans* overexpressing ADH-1. (A-F) Error bars denote SEM. ns= not significant, *p<0.05, **p<0.01, ***p<0.001, ****p<0.0001. (A-D) *daf-2i* = *daf-2* RNAi, *hlh-30i* = *hlh-30* RNAi, *adh-1i* = *adh-1* RNAi, *let-363i* = *let-363* RNAi. All experiments were performed using *E. coli* XU363 carrying L4440 (empty vector) or L4440 + the gene of interest.

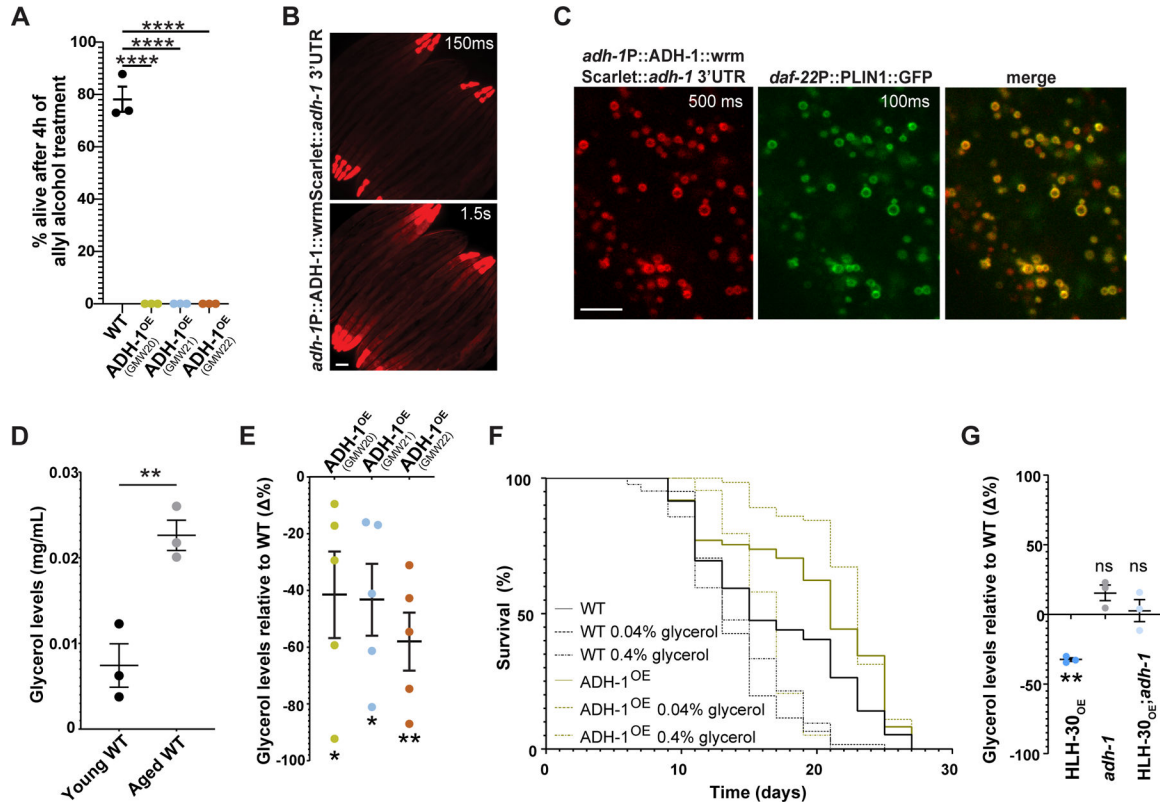


Figure 3. *adh-1* extends lifespan by preventing the accumulation of the aging-promoting metabolite glycerol. (A) ADH-1^{OE} strains are hypersensitive to allyl alcohol, indicating increased *in vivo* alcohol dehydrogenase activity (n=3 biological replicates). (B) Whole-body expression of the ADH-1 protein as observed in N2 *C. elegans* carrying wrmScarlet knocked-in in-frame in the *adh-1* locus via CRISPR/Cas9 (scale bar = 100µm). Two exposure times of the same image are depicted. At the 1.5s exposure time, muscle and intestinal signals are visible. See also Figure S4A-B for additional information on the anatomical localization of ADH-1. (C) ADH-1 co-localizes with intestinally expressed *D. melanogaster* perilipin, a lipid droplet marker expressed from the integrated transgene P*daf-22*::PLIN1::GFP³¹ (scale bar = 5µm). Exposure times are depicted. See Figure S4C for autofluorescence control. (D) Wild type worms accumulate glycerol as they age. Young corresponds to day-1 adult, and aged corresponds to day-8 adult, the latest day we can harvest live worms free of contaminating dead worms (n=3 biological replicates). (E) Three independent ADH-1^{OE} lines show decreased glycerol levels relative to wild type (n=5 biological replicates). (F) ADH-1^{OE} animals are resistant to the pro-aging effect of glycerol (representative of three biological replicates; see Data S1K & Data S1L). (G) Loss-of-function mutation of *adh-1* suppresses the otherwise low glycerol levels observed in HLH-30^{OE} animals. Statistical significance relative to wild-type controls (n=3 biological replicates). (A-G) Error bars denote SEM. ns= not significant, *p<0.05, **p<0.01, ***p<0.001, ****p<0.0001. All experiments (except the glycerol supplementation experiment) were performed using *E. coli* XU363 carrying L4440 (empty vector). The glycerol supplementation experiment was performed using *E. coli* OP50 bacteria.

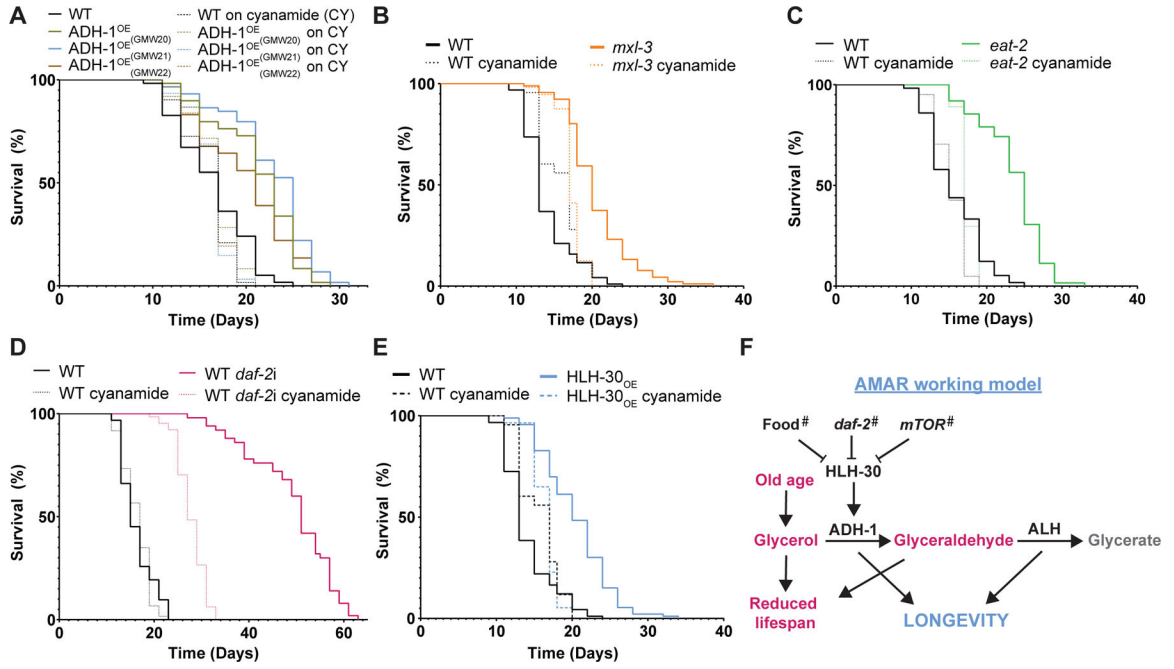


Figure 4. *adh-1* mediated lifespan requires aldehyde dehydrogenase activity.

(A-E) Treatment with the aldehyde dehydrogenase inhibitor cyanamide rescues the extended lifespan driven by (A) ADH-1^{OE} (GWM20–22 are three independent ADH-1^{OE} lines), (B) *mxl-3* mutation, (C) Caloric restriction (*eat-2* mutation), (D) reduced insulin sensitivity (*daf-2* RNAi), and (E) HLH-30^{OE}. See also Data S1F, Data S1H, Data S1I, and Data S1M. (F) Working model of the Alcohol and aldehyde dehydrogenase-Mediated Anti-aging Response (AMAR= immortal in Sanskrit). # Indicates that it remains to be defined how the three inhibitors of HLH-30 tested here (food, the insulin receptor DAF-2, and mTOR) interact among them (or not) to regulate HLH-30 activity. (A-F) Error bars denote SEM. ns = not significant, *p<0.05, **p<0.01, ***p<0.001, ****p<0.0001. All experiments were performed using *E. coli* XU363 carrying L4440 (empty vector) or L4440 + the gene of interest.

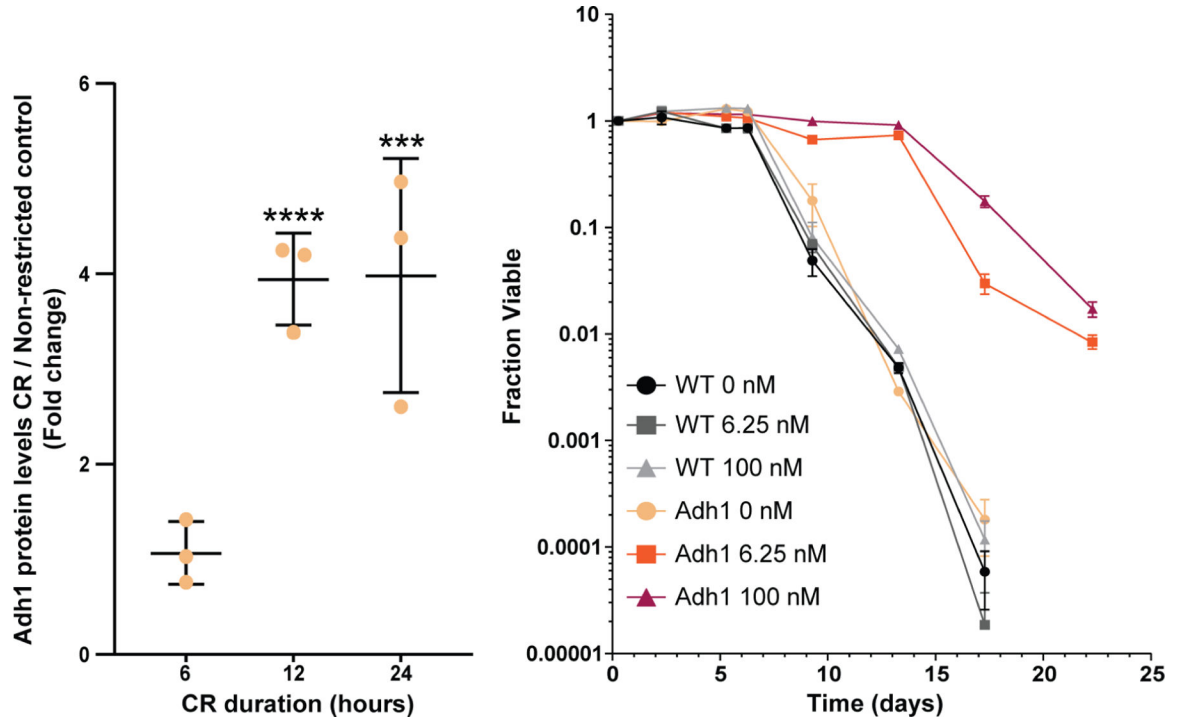


Figure 5. *Adh1* is induced upon caloric restriction and is sufficient to extend chronological lifespan in yeast.

(A) *Adh1* protein levels are increased in calorically restricted (CR) compared to non-restricted yeast as assessed by Western blot. CR duration indicates time since entering the diauxic shift (n=3 biological replicates). (B) *Adh1* overexpression extends yeast chronological lifespan under non-restricted conditions (representative of n=3 biological replicates). Two different doses of estradiol were added to cultures to induce *Adh1* expression. See also Figure S5. (A-B) Error bars denote SEM. *p<0.05, **p<0.01, ***p<0.001, ****p<0.0001.

KEY RESOURCES TABLE

REAGENT or RESOURCE	SOURCE	IDENTIFIER
Antibodies		
Rabbit anti-LGG-1	Ke et al, 2020 ⁷¹	N/A
Rabbit anti-Adh1 (for yeast ADH1 western blotting)	Rockland Immunochemicals	Cat #: 200-4143-0100
Mouse anti-tubulin	DSHB	Cat #: 4A1-s
Rat anti-alpha-tubulin	Invitrogen	Cat #: MA1-80017
Alexa Fluor 800cw goat anti-rabbit	Li-cor	Cat #: 926-32211
IRDye 800cw goat anti-mouse	Li-cor	Cat #: 92632210
HRP-conjugated anti-rabbit IgG	Promega Corporation	Cat #: W4018
HRP-conjugated anti-rat IgG	Abcam	Cat #: ab6734
Alexa Fluor 594 goat anti-rabbit	Invitrogen	Cat #: A11012
Bacterial and Virus Strains		
<i>E. coli</i> strain OP50	CGC	N/A
<i>E. coli</i> strain XU363	CGC	N/A
Chemicals, Peptides, and Recombinant Proteins		
5-fluoro-2-deoxyuridine (FUDR)	Research Products International	Cat #: F10705-1.0
Chloroquine Diphosphate Salt	Sigma-Aldrich	Cat #: C6628
Cyanamide	Sigma-Aldrich	Cat #: 187364-5G
Glycerol	Fisher BioReagents	Cat #: BP229-1
Allyl alcohol	Thomas Scientific	Cat #: C984Z15/240532-100ML
Carbenicillin, Disodium salt	Genesee Scientific	Cat #: 25-532
TRI Reagent	Molecular Research Center	Cat #: TR 118
FastSYBR Mixture	CoWin Biosciences, Inc.	Cat #: CW0955H
Intercept (PBS) Blocking Buffer	Li-cor	Cat #: 927-70001
Critical Commercial Assays		
ReadiUse TCA Deproteinization Sample Preparation Kit	AAT Bioquest	Cat #: 19501
Glycerol assay kit	R-Biopharm	Cat #: NC9662370
BCA protein assay kit	Fisher Scientific	Cat #: 23227
Deposited Data		
RNA-Seq of human adipose tissue after long term caloric restriction	Armenise et al, 201776	Accession number: GSE95640
DNA microarray of human adipose tissue after long term caloric restriction	Capel et al, 200877	PMID: 18782868
DNA microarray of human adipose tissue after long term caloric restriction	Tareen et al, 202078	Accession number: GSE77962
DNA microarray of human adipose tissue after long term caloric restriction	Capel et al, 200979	Accession number: GSE11975
DNA microarray of human adipose tissue after long term caloric restriction	Mutch et al, 201180	Accession number: GSE24432
DNA microarray of human adipose tissue after long term caloric restriction	Nookaew et al, 201381	Accession number: GSE35710

REAGENT or RESOURCE	SOURCE	IDENTIFIER
DNA microarray of mouse heart tissue after short term caloric restriction	Noyan et al, 201582	Accession number: GSE68646
DNA microarray of mouse adipose tissue after short term caloric restriction	Kim et al, 201683	Accession number: GSE60596
DNA microarray of mouse adipose tissue after long term caloric restriction	Higami et al, 200484	PMID: 14688200
DNA microarray of mouse liver tissue after long term caloric restriction	Mitchell et al, 201685	Accession number: GSE81959
DNA microarray of mouse liver tissue after short term caloric restriction	Tsuchiya et al, 200486	PMID: 15039484
DNA microarray of rat liver tissue after long term progressive caloric restriction	Pohjanvirta et al, 200887	Accession number: GSE9121
DNA microarray of mouse intestinal tissue after long term fasting	Hakvoort et al, 201188	Accession number: GSE24504
DNA microarray of mouse gastrocnemius muscle after long term caloric restriction	Lanza et al, 201289	Accession number: GSE36285
DNA microarray of mouse kidney tissue after long term fasting	Jongbloed et al, 201490	Accession number: GSE52982
DNA microarray of mouse cochlea after long term caloric restriction	Someya et al, 200691	Accession number: GSE4786
DNA microarray of mouse liver tissue after long term caloric restriction	Aon et al, 202092	Accession number: GSE124294
Experimental Models: Organisms/Strains		
<i>C. elegans</i> strain: N2 Bristol	CGC	N/A
<i>C. elegans</i> strain: <i>adh-1</i> (<i>ok2799</i>)	CGC	N/A
<i>C. elegans</i> strain: <i>mxl-3</i> (<i>ok1947</i>)	CGC	N/A
<i>C. elegans</i> strain: <i>atg-18</i> (<i>gk378</i>)	CGC	N/A
<i>C. elegans</i> strain: <i>eat-2</i> (<i>ad456</i>)	CGC	N/A
<i>C. elegans</i> strain: OP433 [<i>hlh-30::TY1::EGFP::3xFLAG + unc-119(+)</i>]	CGC	N/A
<i>C. elegans</i> strain: MAH235 (sqIs19 [<i>hlh-30p::hlh-30::GFP + rol-6(su1006)</i>])	CGC	N/A
<i>C. elegans</i> strain: MAH240 (sqIs17 [<i>hlh-30p::hlh-30::GFP + rol-6(su1006)</i>])	CGC	N/A
<i>C. elegans</i> strain: PHX2365 gene knock-in (<i>adh-1P::ADH-1::wrmScarlet::adh-1</i> 3' UTR)	This study	N/A
<i>C. elegans</i> strain: GMW20 integrated arrays backcrossed 3x (<i>adh-1P::ADH-1::wrmScarlet::adh-1</i> 3' UTR)	This study	N/A
<i>C. elegans</i> strain: GMW21 integrated arrays backcrossed 3x (<i>adh-1P::ADH-1::wrmScarlet::adh-1</i> 3' UTR)	This study	N/A
<i>C. elegans</i> strain: GMW22 integrated arrays backcrossed 3x (<i>adh-1P::ADH-1::wrmScarlet::adh-1</i> 3' UTR)	This study	N/A
<i>C. elegans</i> strain: XD3971 (xIds143[<i>Pdaf-22::PLIN1::GFP; rol-6(su1006)</i>])	Liu et al, 2014 ³¹	N/A
Yeast strain: Y15090 (<i>MATa/α</i> [<i>HAP1-NatMX-ACT1pr-Z3EV-ENO2term</i>]/ <i>HAP1 ura3 0/URA3[can1 ::STE2pr-SpHIS5]/CAN1 his3 1/his3 1 lyp1 /LYPI</i>)	Calico labs	N/A
Oligonucleotides		
Primers for qRT-PCR, see Table S1	This study	N/A
Software and algorithms		
SPSS	IBM	N/A
GraphPad Prism	GraphPad	N/A

REAGENT or RESOURCE	SOURCE	IDENTIFIER
OASIS 2	Han et al, 2016 ⁷⁰	N/A

Author Manuscript

Author Manuscript

Author Manuscript

Author Manuscript